A Study on the Design of Electromagnetic Valve Actuator for VVT Engine

Seung-hyun Park*
Graduate school, Department of Mechanical Engineering, Ajou University, Kyunggi-do 442-749, Korea
Dojoong Kim
Department of Mechanical and Automotive Engineering, University of Ulsan, Ulsan 680-749, Korea
Byungohk Rhee, Jaisuk Yoo, Jonghwa Lee
Department of Mechanical Engineering, Ajou, University, Kyunggi-do 442-749, Korea

Electromagnetic valve (EMV) actuation system is a new technology for improving fuel efficiency and at the same time reducing emissions in internal combustion engines. It can provide more flexibility in valve event control compared with conventional variable valve actuation devices. The electromagnetic valve actuator must be designed by taking the operating conditions and engine geometry limits of the internal combustion engine into account. To help develop a simple design method, this paper presents a procedure for determine the basic design parameters and dimensions of the actuator from the relations of the valve dynamics, electromagnetic circuit and thermal loading condition based on the lumped method. To verify the accuracy of the lumped method analysis, experimental study is also carried out on a prototype actuator. It is found that there is a relatively good agreement between the experimental data and the results of the proposed design procedure. Through the whole speed range, the actuator maintains proper performances in valve timing and event control.

Key Words: Electromagnetic Valve(EMV) Actuator, Design by Lumped Method Analysis, Valve Dynamics, Electromagnetic Circuit, Thermal Loading, Prototype Actuator

Nomenclature

m : Moving mass [kg]
K : Equivalent spring stiffness [N/mm]
N : Engins speed [rpm], coil turn number
l : Length [mm, m]
t : Thickness[mm]
F : Force [N]
$\ddot{y}$: Valve, armature acceleration [m/sec^2]
X, x : Position, air gap [mm]
H : Magnetic field intensity [A/m]
B : Magnetic flux density [Gauss]
i, I : Current [Ampere]
v, V : Voltage [volt], volume [m^3]
R : Resistance [Ω]
L : Inductance [Henry]
P : Power [W]
f : Frequency [Hz]
d : Diameter [mm]
k : Thermal conductivity [W/m℃]
h : Heat transfer coefficient [W/m^2℃]
C : Thermal capacity [kJ/kg℃]
τ : Travel time of valve, armature [sec]
μ_0 : Permeability of free space [H/m]
θ : Valve angle, duration [degree]
η : Efficiency
ϕ : Magnetic flux [Wb]
λ : Magnetic flux linkage [Wb·turn]

* Corresponding Author,
E-mail : shpark-h@hanmail.net
TEL : +82-31-219-2351; **FAX** : +82-31-213-7108
Graduate school, Department of Mechanical Engineering, Ajou University, Kyunggi-do 442-749, Korea.
(Manuscript **Received** June 12, 2002; **Revised** December 6, 2002)

Subscripts

v_dur : Valve open duration
int_v : Intake valve
p_spr : Plunger or actuator spring
arm : Armature
sol : Solenoid
fric : Friction
m : Mean, average

1. Introduction

Conventional mechanical valve train systems generally have fixed values for valve lift and valve event timing and duration. These fixed valve events represent a compromise among the conflicting requirements for various operating conditions. Freedom to optimize all parameters of valve motion for each engine operating condition without compromise is expected to result in better fuel economy, higher torque and power, improved idle stability, lower exhaust emissions and a number of other benefits and possibilities. The expected improvements associated with optimization of each aspect of valves are reviewed in the following research papers.

Controlling the engine load by early or late intake valve closing largely eliminates the pumping loss and improves fuel efficiency (Michael M. Schechter, 1996). Dresner et al. reported that the early closure of the intake valve permitted it to reach lighter loads than it was possible with late closing, without significant deterioration of combustion (Dresner and Barkan, 1989). And Sono et al. also reported satisfactory combustion stability at very light engine load of near 2 bar IMEP with unthrottled operation achieved via early intake closing and other enhancements (Sono and Umiyama, 1994). To achieve good cycle efficiency, a very fast burn rate that is supported by a significant amount of turbulence and mixing is required. The higher air velocity increases the flame expansion speed, and it contributes to reduced combustion delay and period (Joo and Chun, 2000). Dresner, Urata, Kreuter and their co-researchers showed that torque can be increased over either the entire or some range of the engine speed by optimizaing valve timing and lift (Urata and Umiyama, 1993).

The optimized expansion ratio can be achieved by proper exhaust valve open timing. Stein et al. used simultaneous retard of intake and exhaust camshafts at part loads to delay valve overlap for increased residual gas fraction, and late intake closing to reduce compression work. In their research, HC and NOx emissions here reduced by up to 12 and 15% respectively (Stein and Leone, 1995). Ahmad classified the categories of VVT (Variable Valve Timing) or VVA(Variable Valve Actuation) system according to the level of sophistication into five types (Ahmad and Theobald, 1989). The early stage of developing process performs a phase shift of camshaft or changes the camlobe to achieve optimized valve timing, lift, and duration. Numerous camshaft-based variable valve mechanisms have been developed. But for this system, individual control of valve timing and other control parameters is seriously restricted by mechanical camshaft system.

Electrohydraulic and Electromagnetic type VVT system, the most flexible devices that give variable lift, duration, and phasing are considered to offer a total valve motion control. Between them, the electromagnetic device has relatively simple structure, and also need fewer design changes of existing engines.

The electro-magnetically controlled system of variable valve actuation consists of intake or exhaust valve, springs, and electromagnets that maintain the close and open positions. The valve is actuated by the motion of the armature between two E-shaped magnetic cores, where the two valve springs fix the neutral position of the armature at the center of the air gap. As a part of the mass-spring resonance system, the armature can swing from one side to the other of the air gap. The magnetic force holds the armature at the extreme positions and provides the energy needed to overcome resistance due to friction and cylinder pressure at exhaust valve open. Figures 1 and 2 show the operation concept and a typical profile of the valve movement, respectively.

Electromagnetic VVT systems have many benefits mentioned above, but much time and efforts

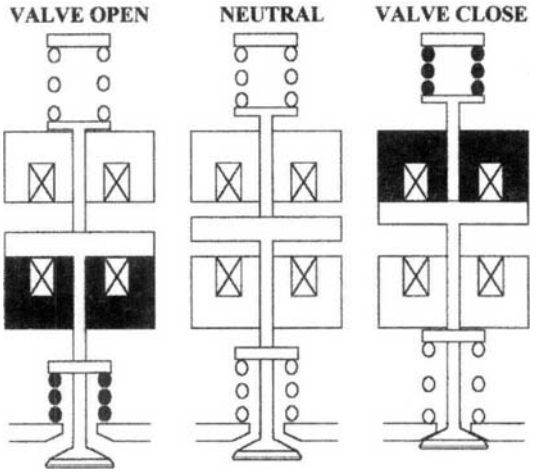

Fig. 1 Schematic diagram of operational procedure of EMV actuator

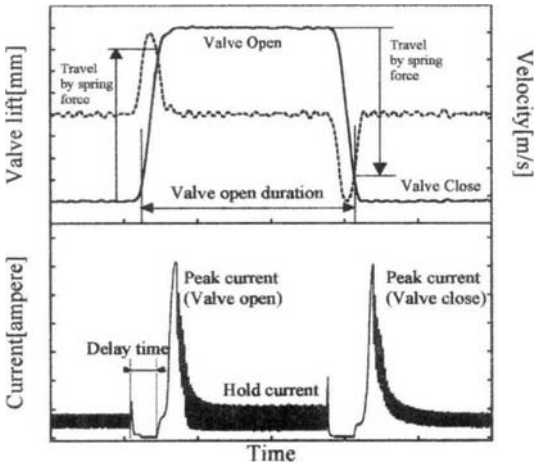

Fig. 2 Typical valve and current profile of EMV actuator

are required in actuator design that is optimized for the given engine. It is mainly caused by the dynamic characteristic of the valve movements and nonlinear electromagnetic characteristics. Also the engine operating and geometric conditions that include valve pitch, stroke, and head cover height exert a significant influence on the actuator design.

This paper presents the design parameters at early stages of actuator design, and describes an effective procedure to apply to the actuator design.

2. Design Parameters for Engine Application

2.1 Relation of "moving mass/spring stiffness" and engine operating range

For the actuator to be used in conventional engines, the EMV system should be capable of operating at high engine speeds of even above 6000 rpm. The valve travel time ("open to close" or "close to open") can be approximately calculated from the fundamental natural frequency of the mass-spring system (Theobald, 1994).

$$\tau_{TRAVEL}=\pi\sqrt{\frac{m}{K}} \tag{1}$$

The possible combinations of the spring stiffness and the moving mass are determined by the valve open duration and maximum operating speed as follows.

$$\frac{m}{K}=\left(\frac{60\times\theta_{OPEN}}{\pi\times N\times 720}\right)^2 \tag{2}$$

For example, at the engine speed of 6000 rpm and valve open duration of 275 crank angle, the corresponding m/K ratio is 1.48×10^{-6} [kg·m/N]. In this case, the natural frequency of the system is 130.8 [Hz], and the valve travel time (open to close, or close to open) is 3.82 [ms]. In order to reduce the minimum valve open duration, or in order to be used in higher engine rotational speed, m/K ratio must be decreased.

The moving mass of the actuator is composed of the following components.

$$Moving\ mass = armature + valve + \frac{1}{3}(plunger + valve)\ springs + stems \tag{3}$$

The valve and valve spring masses in Eq. (3) are determined by the engine configuration. Because a proportion of the plunger spring in the total moving mass is relatively small (3~5%), it can be assumed to be the same with that of the valve spring without incurring a significant error. And, because the actuator stems are designed from the structural point of view, the mass of the stems can be determined separately. However, the moving mass of the armature must be carefully

determined because it comprises the biggest portion in the total moving mass and also has a great influence on the magnetic force of the electromagnets. The sectional area of the armature limits the maximum magnetic flux that flows in the magnetic circuit. It means that the sectional area needs to be increased for permitting a large flux. Therefore, the dimension of the armature should be determined by considering the design of the electromagnet simultaneously.

2.2 Geometric considerations on target engine

As shown in Fig. 3, the structure of an EMV actuator has two sets of electromagnets, two springs, and a casing that covers all of these components.

The effect of engine configuration for the actuator to be adopted, especially that of the cylinder head configuration, on the actuator design is summarized as follows.

(1) Valve pitch, valve angle : Valve pitch is the distance between the centers of the adjoining valves, and it limits the maximum width of the actuator. Valve angle is the interior angle of the intake and exhaust valve. It limits the installation height and position with head cover.

(2) Height of head cover : The cover height of the head is limited by car hood and restricts the installation height of the actuator itself.

The size of the electromagnet is proportional to the magnitude of the electromagnetic force. So the geometrical condition of engine is related with the maximum magnetic force that the actuator can exert. Hence, it is proper to consider a shape of a rectangular parallelepiped to obtain the maximum volume.

The configurations of the engine valve train used in the development of the EMV system are as follows.

1997cc, DOHC (using only #3 cylinder)
- Valve pitch : 37 mm
- Valve angle : 25.5
- Intake valve angle : 12.4
- Diameter of intake valve : 32 mm
- Mass of intake valve : 43.1 gram
- Intake valve length : 187.4 mm
- Intake total height : 312 mm
- Diameter of exhaust valve : 27.4 mm
- Mass of exhaust valve : 43 gram
- Valve spring stiffness : 30 [N/mm]
- Mass of valve spring : 40.8 gram

2.3 Geometric relations of electromagnet

Figure 4 shows the cross section of the EMV actuator with the 'E' shaped laminated core plates. The engine geometry can be incorporated in the actuator design by applying the following equations.

As an example of the intake valve actuator, the valve pitch limits the dimension 'E' in Figure 4.

$$E=4w+2w_p \leq \textit{valve pitch} \tag{4}$$

The depth of core sheets and the solenoid height are restricted by the valve length and the valve angle as given by Eqs. (5) and (6).

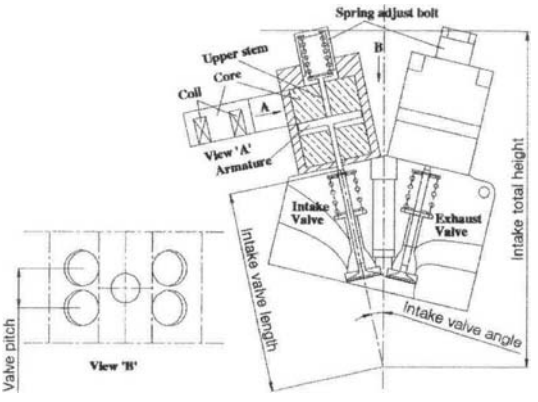

Fig. 3 Relation of engine geometry and EMV actuator design

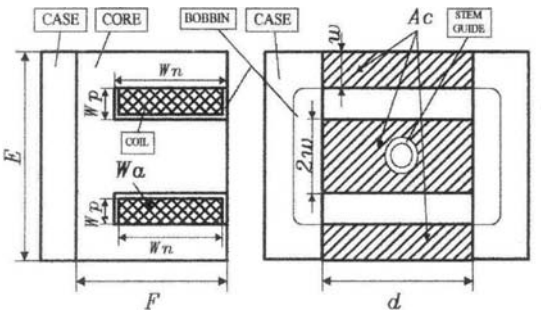

Fig. 4 Dimension of laminated 'E' shaped core

$$d \le 2 \times l_{int\_v} \times \tan(\theta_{int\_v}) - 2(t_{case} + E/6) \quad (5)$$

$$2F \le \frac{l_{total}}{\cos(\theta_{int\_v})} - (l_{int\_v} + l_{p\_spr} + l_{v\_stroke} + t_{arm} + 2 \cdot t_{case}) \quad (6)$$

$$W_a = (w_p - t_{bobbin}) \times (w_n - 2t_{bobbin}) = w_p' \times w_n' \quad (7)$$

W_a in Eq. (7) is the window area to be filled with coil and resin. Eq. (8) represents the acting area of the magnetic flux.

$$A_c = 4w \times S \cdot d,\ S = t_{core}/(t_{core} + t_{coating}) \quad (8)$$

S is used to consider the coating thickness of the laminated plates. Geometric relation of the cross section in Figure 4 gives the relation between the number of coil turns and the diameter (d_o) of the coated coil. Number of coil turns which can be wound in the window area W_a can be approximated by Eq. (9) (Chung, 1996).

$$N \cong \frac{2}{\sqrt{3}} \left(\frac{w_n' \cdot w_p'}{d_o^2} - \frac{w_n'}{d_o} \right) \times \eta_{turn} \quad (9)$$

Here, η_{turn} is the efficiency of the coil winding on the bobbin, which can be significantly influenced by different winding methods. Because the bobbin has a rectangular shape in this study, the efficiency is relatively low compared with that of the circular shaped bobbin. When the coil is wound by a manual winding machine, the efficiency does not exceed approximately 80~85%.

3. Modeling for Dynamic, Magnetic Force, and Heat Transfer Analysis

3.1 Dynamic analysis model

The simulation model is used in confirming the actuator design by estimating the effect of the design parameters, operating parameters, and external disturbances. The equations of motion are derived from the free body diagram shown in Figure 5.

Assuming that the valve and armature move together as one body, from the Newton's law of motion, the equation of motion of the moving mass is derived as follows (Ogata, 1998)

$$m\ddot{y} = F_{spr} + F_{stop1} - F_{sol1} - F_{stop2} + F_{sol2} \pm F_{fric}. \quad (10)$$

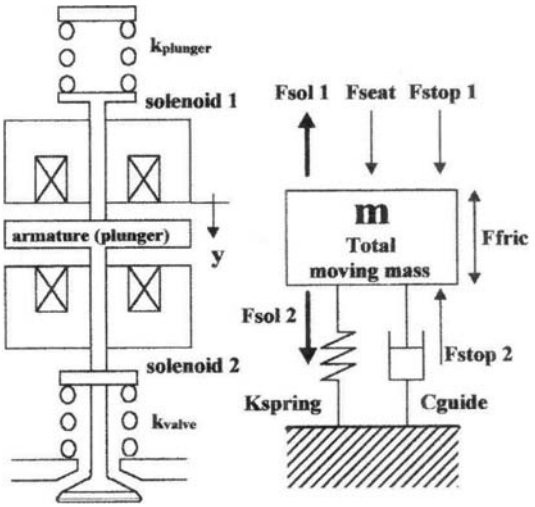

Fig. 5 Dynamic model of EMV actuator

To represent the swinging operation of the moving mass between the two springs, contact forces at the extreme positions in Eq. (10) can be neglected. The swinging motion is simply expressed by

$$m\ddot{y} = F_{spr} - F_{sol1} + F_{sol2} \pm F_{fric} \quad (11)$$

where

$$F_{spr} = K\left(\frac{1}{2}stroke - y\right),\ K = k_{plunger} + k_{valve}$$

$$F_{sol1},\ F_{sol2} = f(N \cdot i,\ gap)\ \textit{at static condition.}$$

The solenoid force can be estimated by the FEM or simply lumped method that is explained in the following section.

In practical cases, however, the stops may also have some elastic effects that result in bouncing of the armature and valve at the ends of their travel. And, if the armature stem always maintain contact with the valve stem, the valve will not be closed. To prevent the above phenomenon, maintaining a proper valve clearance is necessary. This clearance in turn affects the valve acceleration. Furthermore, wide clearance causes noise and vibration, while narrow clearance causes valve overheating and leakage of the compressed gas between the valve and valve seat (Chun and Lee, 2000). Therefore, it is highly recommended to besure a proper clearance between the armature and valve stems for prevent the above problem. To solve the problem, the valve dynamics and the

heat transfer mechanisms of the actuator need to be considered simultaneously.

The movement of the valve can be determined by the force of electromagnets and springs as given in Eq. (11). While the magnetic force has a nonlinear characteristic, the force by compressed spring has a linear characteristic according to the air gap. The two characteristics are schematically explained in Figure 6.

◆ X2~X2′: At the early stage of initialization, the strong peak currents are supplied to the two electromagnets alternately as resonance frequency of the system (3~5th/electromagnet).

$$\frac{d(F_{sol}-F_{spr})}{dX}(X_0, X_1, X_2)>0$$

◆ X1~X1′: It indicates the mean oscillation amplitude by the spring force from the opposite extreme position during normal operation.

$$\frac{d(F_{sol}-F_{spr})}{dX}(X_1)>0, \quad \frac{d(F_{sol}-F_{spr})}{dX}(X_2)<0$$

◆ Fmo, Fso: Magnetic force and compressed spring force at extreme positions (minimum air gap.).

$$F_{mo}>F_{so}$$

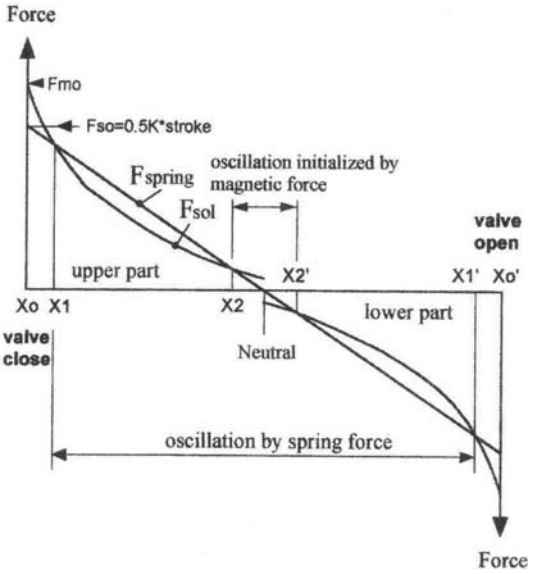

Fig. 6 Sketch for determining equilibrium points for EMV actuator system

Referring to Figures 1 and 6, the armature oscillates within a certain region by the spring action. In the ideal case, the width of oscillation zone is the same as that of the valve stroke. But it is decreased by the influence of friction in real cases. The decrease in amplitude is about 10~20% of the total valve stroke in a lubricated condition. Therefore, the driving force is supplied from the magnetic force near the extreme positions. The design of two key factors, that is, the electromagnetic force and spring force according to air gap, can be determined from the operating range of the target engine.

3.2 Magnetic force

To make the analysis of Figure 7 more tractable but still quite accurate, it is conventional to make the following assumptions (Woodson and Melcher, 1990):

1) The permeability of the magnetic material is high enough to be assumed infinite.

2) The air gap length 'x' is assumed to be small compared with the transverse dimension, so that the fringing at the gap edges can be ignored.

3) Leakage flux is assumed to be negligible, that is, appreciable flux passes through the magnetic material only except for the air gap.

From the equations which describe the field in an electromagnetic system,

$$H_1x+H_2x=Ni \tag{12}$$

$$\mu_0H_1(2w_1d)-\mu_0H_2(2w_2d)=0. \tag{13}$$

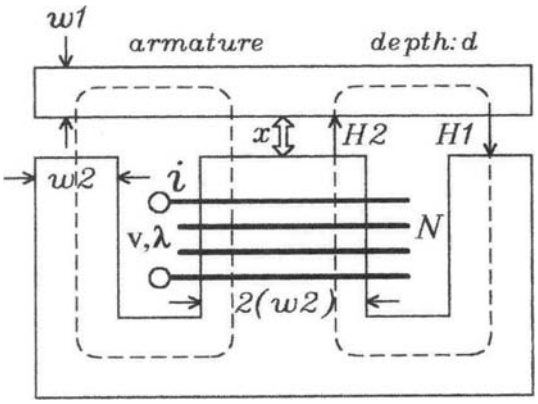

Fig. 7 The magnetic field system of electromagnet

If $w_1=w_2=w$, combine (12) and (13) to obtain

$$H_1=H_2=\frac{Ni}{2x}. \tag{14}$$

The flux through the center leg of the core is simply the flux crossing the air gap x,

$$\phi=\mu_0 H_2(2wd)=\frac{wd\mu_0 Ni}{x}. \tag{15}$$

Over a surface enclosed by the wire of the N-turn winding, we obtain the flux linkage given by

$$\lambda=N\phi=\frac{wd\mu_0 N^2 i}{x} \tag{16}$$

where

$$\frac{wd\mu_0 N^2}{x}=L(x),\ \lambda=L(x)\cdot i.$$

And the magnetic coenergy is

$$W_m'=\int_0^i \lambda(i,x)\cdot di=-\frac{1}{2}\frac{L_0 i^2}{2x/x_0}$$
$$L_0=\frac{wd\mu_0 N^2}{x_0},\ x_0;\ \textit{minimum air gap.} \tag{17}$$

The force source applied to the mechanical node x is

$$F_{sol}=-\frac{1}{2}\frac{L_0 i^2}{x^2/x_0} \tag{18}$$

When we assume that the current i and displacement x are specified functions of time and apply Kirchhoff's voltage law to the electrical loop, we can evaluate the terminal voltage of Figure 7 as

$$v=iR+L(x)\frac{di}{dt}+i\frac{dL}{dx}\frac{dx}{dt}$$
$$=iR+\frac{L_0}{x/x_0}\frac{di}{dt}-\frac{L_0\cdot i}{x^2/x_0}\frac{dx}{dt}. \tag{19}$$

It can be shown that the power consumption of the electromagnet including the core loss is given by

$$P_{total}=P_{cu}+P_{sol}+P_{core}=vi$$
$$=i^2R+\frac{L_0\cdot i}{x/x_0}\frac{di}{dt}-\frac{L_0\cdot i^2}{x^2/x_0}\frac{dx}{dt}$$
$$+V_{core}\,f\cdot\oint_{dynamic} HdB. \tag{20}$$

The electrical power that is supplied to an electromagnet is consumed by the resistance heat generation of coil (Pcu) and magnetic force (Psol), and core loss (Pcore=hysterisis loss+ eddy current loss) of the material. The core loss can be calculated by multiplying the volume of the electromagnet, the area of the dynamic B-H loop that follows the material characteristics, and the frequency of time varying flux (f) (Sen, 1987). For practical applications, the core loss of laminated thin core plates is represented by $P_{core}=A\cdot f^{\alpha}\cdot B_g^{\beta}$, and the coefficients A, α and β depend on material and thickness (McLyman and Colonel, 1997).

3.3 Heat transfer

Figure 8 shows the heat source and its transfer path in the EMV system. Heat generation in the EMV actuator is mostly due to the coil resistance, core hysterisis and eddy current loss. Because the temperature increase of the coil can be a major cause of the coil damage, the heat generation must be suppressed and the generated heat must be

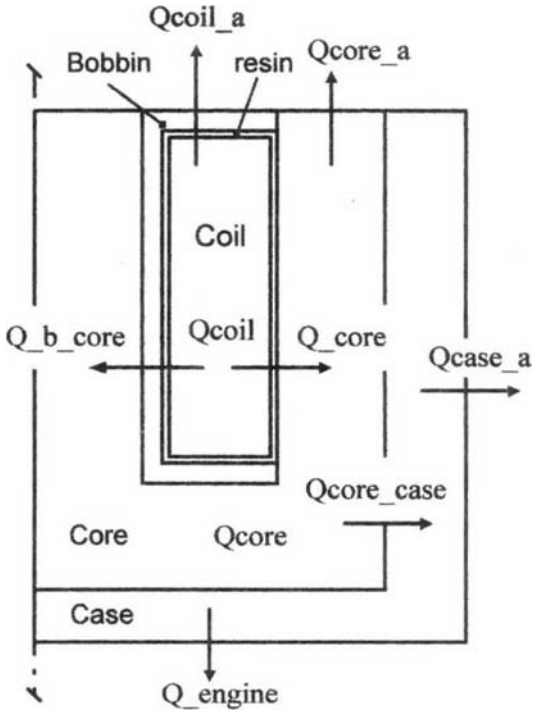

Fig. 8 Heat transfer path of EMV actuator

effectively scattered.

Lumped method is used to derive the heat transfer Eq. (21), which considers some components with relatively large heat capacity such as solenoid coil, core and casing.

$$[(mC)_{coil}]\left(\frac{dT_{coil}}{dt}\right) = \dot{Q}_{coil} - \dot{Q}_{coil\_a} - (\dot{Q}_{\_b\_core} + \dot{Q}_{\_core}) - \dot{Q}_{coil\_case} \tag{21}$$

where,

$$\dot{Q}_{coil} = I(t)^2 \cdot R_{coil},$$
$$R_{coil} = R_0(1 + \alpha_1(T_{coil} - T_o))$$
$$R_0 = \frac{4\rho N \cdot l_m}{\pi d_c^2} \tag{22}$$

Eq. (22) represents the heat generation rate by the coil resistance, and the coefficient is the resistivity of the coil material, which is 1.72×10^{-8} [m] for copper. The coefficient 1 is the temperature coefficient of the resistance, and that of copper is 0.00393 [1/℃] at 20 ℃.

Equation (23) represents the heat transfer rate through the upper bobbin from the coil to the surrounding air.

$$\dot{Q}_{coil\_a} = \frac{1}{R_{coil\_a}}[T_{coil} - T_{air}] \tag{23}$$

where,

$$R_{coil\_a} = \frac{1}{A_{bobbin}}\left(\frac{l_{resin}}{k_{resin}} + \frac{l_{bobbin}}{k_{bobbin}} + \frac{1}{h_{air}}\right).$$

The third and forth terms on the right side of Eq. (21) are the heat transfer terms from the coil to the core. And, the end of the right side of Eq. (21) is heat release to the case which directly contacts the coil normal to paper.

Heat transfer model of the core is summarized by Eq. (24), which considers the heat generation due to the core loss and heat transfer through the casing.

$$[(mC)_{core}]\left(\frac{dT_{core}}{dt}\right) = \dot{Q}_{\_b\_core} + \dot{Q}_{\_core} + \dot{Q}_{core} - \dot{Q}_{core\_a} - \dot{Q}_{core\_case} \tag{24}$$

where $\dot{Q}_{core}$ is the heat generation due to the core loss.

$$[(mC)_{case}]\left(\frac{dT_{case}}{dt}\right) = \dot{Q}_{coil\_case} + \dot{Q}_{core\_case} - \dot{Q}_{case\_a} - \dot{Q}_{engine} \tag{25}$$

Generated heat at the coil and core is mostly scattered through the casing to the cylinder head and surrounding air as expressed in Eq. (25). Cylinder head temperature was calculated by using the engine component temperature prediction model (Kaplan, 1990).

4. Design Procedure of EMV Actuator

4.1 Determination of the natural frequency of EMV actuator

To determine the natural frequency of the EMV actuator in the operating region of conventional spark ignition engines, the design scope of the moving mass and spring stiffness is calculated by using Eqs. (1)~(3). Figure 9 shows the design scope. The valve travel time is proportional to the square root of the moving mass, and also inversely proportional to the square root of the spring stiffness. In most cases, the plunger spring does not interfere with design of other parts. Hence, the stiffness of the plunger spring is set to be as high as possible in consideration of the space constraint and material fatigue limit.

4.2 Actuator moving mass vs. engine operating conditions

From Eq. (3), the moving mass is calculated to be about 85.3 grams excluding the armature mass. For the actuator to operate at the engine speed of 6000 rpm with the valve open duration of 250~300 crank angle, the moving mass including the armature must be in the range of 122~176 grams [armature mass: 36.7~90.7 grams]. The upper part of figure 9 shows the valve travel time with respect to the moving mass and spring stiffness. The lower part of figure 9 represents the maximum possible engine operating speed as a function of the moving mass and valve open duration. Equivalent spring stiffness is assumed to be 100 N/mm in the calculation.

The range of the approximate armature mass can be estimated from the following relations. The maximum effective area of core plates is calculated from geometric constraints by applying Eqs. (4) and (5). Because the valve pitch is 37 mm, E in Figure 4 is decided to be 35 mm in

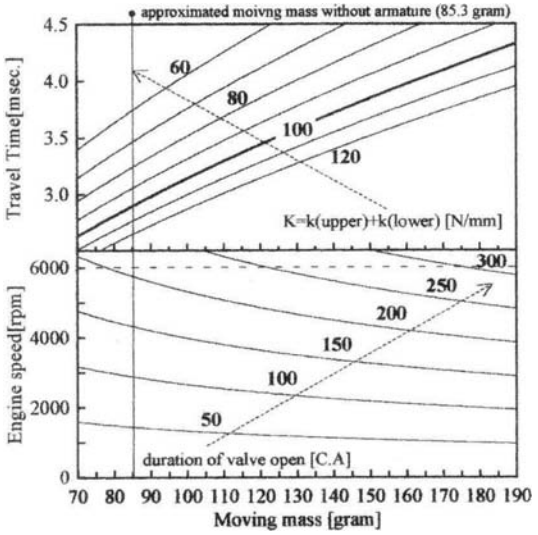

Fig. 9 Relations between actuator design parameters and engine operating conditions

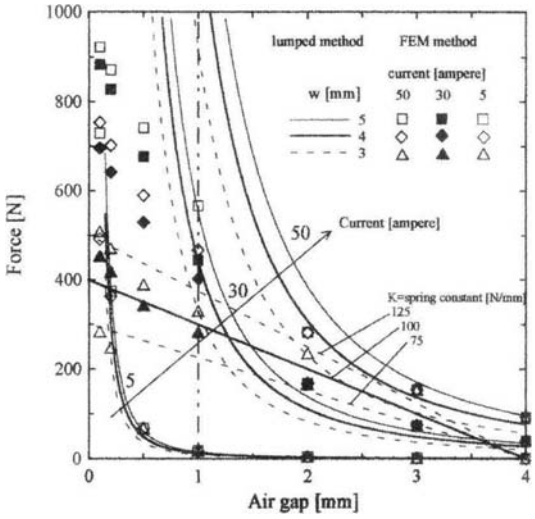

Fig. 10 Electromagnetic force as air gap and thickness of armature by lumped-parameter method and FEM

consideration of the minimum clearance between the actuators. And the depth of core d in Figure 4 is about 50~55 [mm] considering the thickness of the case and coil winding from Eq. (5).

Therefore, the effective area (d·E) of the core plates is calculated to be 1750~1925 mm^2. If the armature material is pure iron, the range of the armature thickness can be estimated from the range of the armature mass. In this case, the thickness of the armature is in the range of 2.7~6.5 [mm] or 2.4~5.9 [mm]. And, the density of pure iron is 7897 [kg/m^3]. That is, the armature thickness can be chosen in the range of 2.4~6.5 [mm] according to the engine head geometry and target operating region.

4.3 Coil diameter and coil turn number

Based on the geometric relations mentioned above, the number of coil turns to be wound can be estimated by using Eq. (6). In the case of the coil diameter, d_o=0.96 (d_i=0.9 mm), 68~73 turns of coils can be wound. If the diameter is 1.06 mm, number of coils to be wound is reduced to 55~58 turns. Because the magnetic force is proportional to the square of the coil turns, there is 37% difference in the magnetic force between the two coils.

4.4 Calculation of the electromagnetic force

Figure 10 shows the result that is calculated from Eqs. (17) and (18) by examining the electromagnetic force as armature's thickness according to air gap. For obtaining better magnetic force characteristics, 0.96 mm coil (do) and coil turn number=70 is used for the calculation.

To examine the level of the current flowing through the coil at places of dynamic importance, we set the initial current condition at 50 [ampere] to actuate the armature by extreme position from the neutral, and the hold current is 5 [ampere] that is to keep armature in extreme position.

The level of the current supplied and the armature thickness can be adjusted by the spring stiffness which is related with engine operating conditions. For higher engine operating speed, the thinner armature and stiffer spring are needed. From the results of Figure 10, we can estimate the optimum design parameters.

From the design process (1)~(4), the basic design parameters are set. For example, the combination of the spring stiffness and moving mass, and electromagnetic force which also can be determined by m/k ratio. The results are plotted in Figures 9 and 10. Therefore, we can simulate the armature and valve movements using system

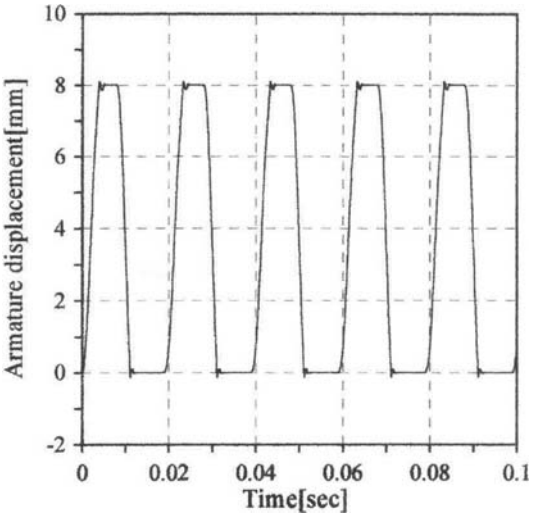

Fig. 11 Simulated armature displacement under pre-designed conditions

dynamics Eq. (10).

The simulation results are plotted in Figure 11. The trace of armature movement and the surging effect are displayed in the figure. Where, the effects of design parameters are simulated with disturbance forces.

4.5 Basic dimension of electromagnet

According to the calculaed result of Figure 10, it needs to supply the current of more than 50 [ampere], which was set the design condition to drive armature from the neutral position in the case of 3 mm thickness of armature. Also, the holding zone is drastically reduced. But for the cases of 4 and 5 mm armatures, the required force to derive the valve from the neutral position is safisfied. However, it is recommended to select the armature of around 4 mm to reduce the valve travel time by decreasing the moving mass.

Symbols in Figure 10 show the calculated results of the electromagnetic forces by the FEM. The magnetic forces from the FEM are considerably different with those from the lumped method in Eq. (18), especially in the extreme region. These differences are related to the permeability of the core and armature materials, which is mentioned in Eq. (18). Because the permeability of pure iron and silicon steel, which is widely used for the core and armature material, is not infinite, saturation phenomenon occurs when the magnitude of the magnetic flux passing through the material exceeds a certain level. The magnetic force that acts the air gap is in proportion to the magnetic flux that flows in the magnetic circuit, but in practical cases, the magnetic force increases along a "S" shape curve. And the slope follows the B-H curve of the material.

But, the flux saturation phenomenon does not occur at the three points, that is, the starting zone, the holding zone and the extreme zone that were referred before. Therefore the calculated results agree well with the two methods.

The selection of the material and the flux sectional area is based on the consideration of the total amount of the magnetic flux density and the core loss in Eqs. (12) and (13). From Eq. (13), the total amount of the magnetic flux that flows section of flux path is equal in all routes which results in the following relation.

$$B_2(w_2d_2)=B_1(w_1d_1)$$

To reduce the eddy current loss, in general, the core is made of laminated thin plates with insulation coating. Because the stem guide, which is made of a non-ferrous material, is located at the center of the core to support the straight motion of the armature and upper stem, the effective cross sectional area of the core is reduced as follows

$$\left((w_2-d_{s\_guide})\times\frac{t_{core}}{t_{core}+t_{coating}}\times d_2\right)\cdot B_2=(w_1d_1)\cdot B_1.$$

Therefore, the size of the cross section is decided carefully to avoid local saturation in consideration of the material characteristics.

Table 1 lists the principle magnetic characteristics of the materials. In this study, Ni-Fe alloy was selected for reducing the core loss, and Si steel was selected by considering valve dynamics and durability. According to table 1, the maximum magnetic flux density of Si steel is higher than that of Ni-Fe alloy, while the permeability that affects the response time and core loss shows the opposite trend (McLyman and Colonel, 1997).

Table 1 The magnetic properties of core and armature materials

	Bmax [G]	Permeability	Remark
1%Si steel	15,200	6,000	Armature
3%Si steel	14,700	12,000	Armature
50%Ni-Fe	14,000	30,000	Core
80%Ni-Fe	6,500	100,000	Core

4.5 Estimation of thermal load on EMV actuator coil

Figure 12 shows the profiles of the current supplied to the coil at various engine speeds.

The current level that is supplied to the electromagnet is controlled by PWM method for improving durability and power consumption economy of the actuator.

Waveform of the current supplied to the electromagnet is a series of peaks and holding currents in a regular succession. After the peak current of 50~60 ampere is supplied, the current suddenly drops to the holding current of less than 5 ampere when the armature contacts the core plate. Therefore, if the engine operating speed or valve travel time increase, heat generaed due to the coil resistance also increases. To reduce the effect of external disturbances, the peak current supply time can be increased, and that may have negative effect on the heat generation.

The generation of heat caused by the current supplied and the coil resistance can be calculated from Eqs. (20) and (22). And the coil resistance is influenced by the coil temperature and the diameter of coil.

The loss can be estimated to be about 10~20% of the total power consumption, and it increases or decreases by the design and operating conditions. Furthermore, the heat resistance temperature of the film coating on coil exists in the range of 160~200 ℃ in general, and the bobbin and the resin, which has relatively low heat conductivity, encloses the coil. Therefore, the heat from the coil cannot be emitted effectively from the coil to the environment.

In particular, the upper magnet has no direct contact with the cylinder head unlike the lower magnet, and the heat from the upper solenoid

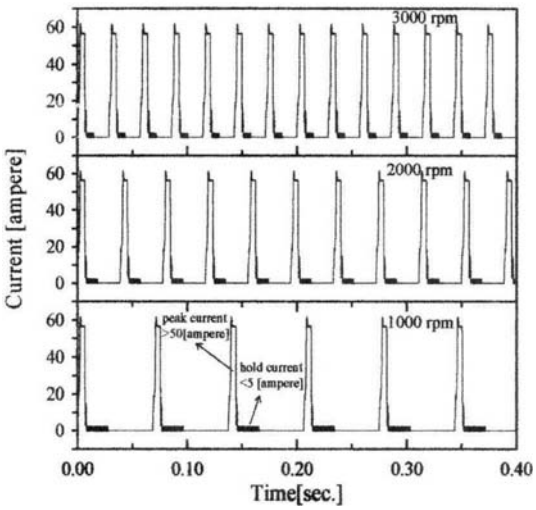

Fig. 12 Current profiles of the EMV actuator

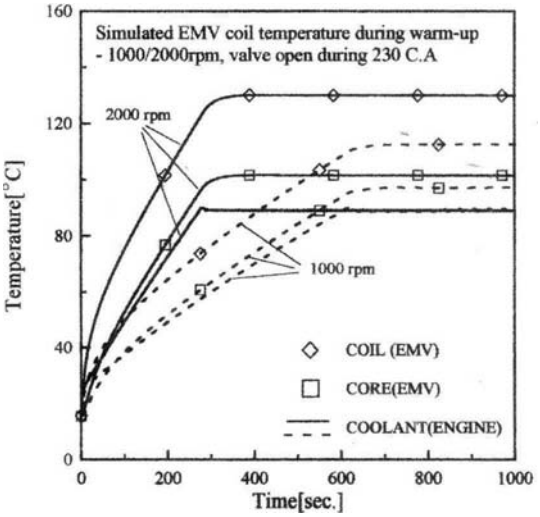

Fig. 13 Simulated EMV actuator temperature during engine warm-up

coil must be transferred to the surrounding air. However, because the actuator is located just under the hood, where airflow is relatively weak, serious heating over problem may develop at high-speed operations. Therefore, the thermal condition of the engine needs to be considered for the determination of the design and the operating condition of the EMV actuator.

Figure 13 shows the simulation results of the EMV actuator temperature based on the heat transfer model and the engine component tem-

perature prediction model. The simulation results are calculated with the following conditions : engine speed of 1000 rpm, intake pressure of 0.35 bar, theoretical air/fuel ratio. To verify the actuator performance in an extreme condition, supply time of the peak current is increased by 50% during the coil temperature calculation. In full warm-up conditions, the difference between the coil and coolant temperatures is maintained at about 25℃ (1000 rpm) ~40℃ (2000 rpm).

Figure 14 compares the test results with the analysis results shown in Figure 10 for the case of 4 mm armature thickness. The trend in the magnetic force obtained by testing with respect to that of the air gap is similar to that of the analysis. But, there is an error of approximate 100 N between the test and analysis results of the magnetic force around the catching zone of 1 mm air gap. The difference seems to include the analysis error and the manufacturing error in the flatness of the armature and core planes. Judging from the test results, the armature-catching zone must be set with an air gap of less than 1 mm for safe operation. Because the actuator developed in this study has about 3.3 mm free oscillation amplitude in lubricated conditions, the catching zone of 1 mm air gap will guarantee the safe operation. Judging from the test result in the proximity zone, the holding current must be bigger than 4 amperes to keep the valve at open or close positions.

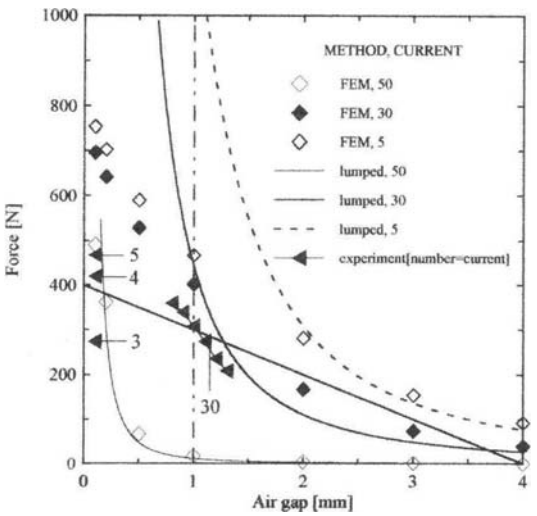

Fig. 14 Electromagnetic force of prototype of EMV actuator

5. Conclusions

The electromagnetic valve actuator must be designed by considering of the operating conditions and engine geometry limits of the internal combustion engine. This paper presents a procedure for determining the basic design parameters and dimensions of the actuator from the relations governing the valve dynamics, electromagnetic circuit and thermal loading condition. The following conclusions have been made :

(1) The maximum size of the EMV actuator is limited by the engine geometry including the head cover height that is also restricted by the car hood. Generally, the magnitude of the electromagnetic force generated can be related with the volume of the electromagnet. Therefore, the limitations in the actuator dimension can be estimated from the cylinder head geometry as such valve angle, valve pitch, and the location of spark plug by applying the equations developed in this paper.

(2) The operating condition of the target engine directly affects the natural frequency of the actuator. The EMV actuator can be modeled as a system composed of two electromagnets and a typical spring-mass-damper system. Therefore, the best condition for satisfying the two major characteristics involving the valve dynamics and the electromagnetic force need to be determined. In this paper, a simple and fast method for designing the actuator is proposed, and the results are validated by applying the analytical and experimental methods.

(3) It has an important role in the operation of the intake and exhaust valve by the electromagnet at the beginning of the movement, the catching zone which has the air gap of near 1 mm, and the holding zone which maintains the armature at extreme positions. And the relations of these three points become the major criterion for determing the relation of the electromagnetic and spring forces. Furthermore, the level of the coil current

and the supplying method affects the thermal durability of coil together with engine operating conditions. The simulation results are obtained based on the heat transfer model for prediction of coil temperature under the engine operaing condition.

Acknowledgment

The authors would like to acknowledge the financial support provided by National Research Laboratory project (The Ministry of Science and Technology).

References

Ahmad, T. and Theobald, M. A., "A Survey of Variable Valve Actuation Technology," SAE paper 891674.

Butzmann and Melbert, J., 2000, "Sensorless control of Electro-Mechanical Actuators for Variable Valve Train," SAE 2000-01-1225.

Chun, D. J., Lee, J. K., 2000, "An Analysis of Valve Train Behavior Considering Stiffness Effects," *KSME International Journal*, Vol. 14, No. 3, pp. 283~290.

Chung, J. T., 1996, "A Designof the VCM Coil Diameter of a Rotary Actuator in a Computer Hard Disk Drive," *KSME International Journal*, Vol. 10, No. 1, pp. 22~30.

Dresner, T. and Barkan, P., "A Review of Variable Valve Timing Benefits and Modes of Operation," SAE paper 891676.

Heywood, J. B. 1988, "Internal Combustion Engine Fundamentals," McGraw Hill.

Joo, S. H. and Chun, K. M., 2000, "Swirl Effect on the Flame Propagation at Idle in a Spark Ignition Engine," *KSME International Journal*, Vol. 14, No. 12, pp. 1412~1420.

Kaplan, J. A., 1990, "Modeling The Spark Ignition Engine Warm-Up Process To Predict Component Temperatures," M.I.T.

Katsuhiko Ogata, 1998, "System Dynamics," 3rd edition, Prentice Hall.

Kekedjian, H. and Krepec, T., 1994, "Further Development of Solenoid Operated Gas Injectors with Fast Opening and Closing," SAE paper 940450.

Lewis, R. W., Morgan, K., Thomas, H. R., Seetharamu, K. N., 1996, "The Finite Element Methodin Heat Transfer Analysis," Wiley.

McLyman and Wm. T. Colonel, 1997, "Magnetic Core Selection for Transformers and Inductors," Marcel Dekker.

Michael M. Schechter and Michael B. Levin, "Camless Engine," SAE paper 960581.

Park, S. H. and Lee, J. H., "The Analysis and Experiments for the Design of Electro-mechanical Variable Valve Train System," *KSAE*, Vol. 9, No. 3, pp. 60~67.

Park, S. H. and Lee, J. H., 2002, "The Analytic and Experimental Research on Dynamic Characteristics of EMV System," *KSAE*, Vol. 10, No. 3.

Seely, S., 1962, "Electrical and Electronic Engineering Series," Mcgraw Hill.

Sen, P. C., 1997, "Principles of Electric Machines and Power Electronics," Wiley & Sons, Inc.

Sono, H. and Umiyama, H., "A Study of Combustion Stability of Non-Throttling S. I. Engine with Early Intake Valve Closing Mechanism," SAE paper 945009.

Stein, R., Galietti, K. and Leone, T., "Dual Equal VCT-A Variable Camshaft Timing Strategy for Improved Fuel Economy and Emissions," SAE paper 950975.

Theobald, M. A., 1994, "Control of Engine Load Via Electro-Mechanical Valve Actuator," SAE paper 940816.

Urata, Y., Umiyama, H., Shimizu, K., Fujiyoshi, Y., Sono, H. and Fukuo, K., "A Study of Vehicle Equipped with Non-Throttling S. I. Engine with Early Intake Valve Closing Mechanism," SAE paper 930820.

Woodson, H. H. Melcher, J. R., 1968, "Electromechanical Dynamics," Robert E. Krieger Publishing Company.